Modelling and Control of Non-isolated Efficient Boost Converter with Compact Storage Elements

R.Srimathi † ,S.Hemamalini *
School of Electrical Engineering
Vellore Institute of Technology
Chennai, India- 600127
Email: srimathi.r@vit.ac.in ; hemamalini.s@vit.ac.in

***Abstract*—Energy Storage systems (ESS) is of major concern in grid connected systems. The energy derived from renewable energy sources has to be lifted up and should be stored in ESS. Therefore there is a need to develop a boost converter with high performance and less volume. In this paper a 400W Compact Boost Converter (CBC) is designed and control transfer functions are obtained using Small Signal Modelling (SSM). A hardware prototype and controller using aurdino is developed and implemented. The performance of the controller is validated for any load disturbances. The voltage and current ripple of CBC is one half that of conventional Boost converter. The efficiency of the converter is also increased by 2%.**

***Index Terms*—Energy Storage Systems(ESS), ArduinoAT-Mega328) Microcontroller, Digital PID Controllers, Efficiency.**

I. Introduction

THE Distributed Energy Storage Sytems (DESS) is used in a grid connected Renewable Energy Systems (RES). The fossil fuel prices are increasing day by day due to their depletion and thereby RES such as Solar, Wind, Biomass etc are used widely. However due to their intermittent nature Energy Storage Systems (ESS) is mandatory. Hence there is a demand for developing high power DC/DC converters for ESS [1]–[3]. The DC bus in ESS is an interface between DC-DC converters and the inverter. To regulate the low output voltage from RES, there is a need to develop high power DC-DC boost converter with reduced size, high efficiency and high power capacity [4]–[6].

There are instances where high power, high gain converters and their controllers play important role in power regulation in a DC bus [7], [8]. Transformer based boost converter topologies provide isolation and high gain for grid connected systems [9]. This in turn makes the system bulky and costly. Boost converter with coupled inductors has also been proposed for isolated converters [10]. The non-isolated, transformer less topologies are gaining attraction nowadays. They can provide high conversion ratio, less component count and high efficiency [11], [12]. The main objective of the paper is to present a non isolated DC/DC Boost Converter with low voltage and current ripple, low cost, reduced size. This converter is called as Compact Boost Converter (CBC).

The performance of DC/DC converters can be improved by using a digital controller [13]–[15]. Digital PID controllers are simple and robust. It has good noise tolerance and less maintenance. They also have disadvantages like quantization error, differential linearity error (DNE), integral linearity error (INE)etc. Despite of these errors they are ingenious devices. This paper introduces a CBC with digital redesign approach. The control transfer function derived in continous time domain (Z) by Small Signal Modelling (SSM) is thus converted into discrete time domain (Z).The CBC converter is designed and a hardware prototype of 400W is developed. The converter is operated in Continuous Conduction Mode (CCM) [16]–[18]. In addition, a PID controller is designed for the CBC and is implemented in hardware using Aurdino microcontroller (AT-Mega328) [19]. The performance of CBC is compared with conventional Boost Converter(BC) in terms of load regulation, size of the passive components and efficiency.

II. Operation of Compact Boost Converter

Fig.1 shows the schematic of CBC. This topology consists of two diodes (D_1, D_2) ,two MOSFET's (S_1, S_2), inductor L, and capacitor, C. Inspite of increase in component count for same voltage gain, the size of the converter is reduced to half than the traditional boost converter. The analysis for CBC is done for CCM and the duty cycle D, of the switches are equal. The triggering sequence of the switches, inductor current and the output voltage waveforms of CBC is shown in the Fig.2. There are four modes of operation and the equivalent circuits are shown from Fig.3 to Fig.6. Mode 1 and 3 are termed as charging modes. The inductor, L gets charged during these modes. Modes 2 and 4 are discharging modes where the energy stored in the inductor is delivered to the load.

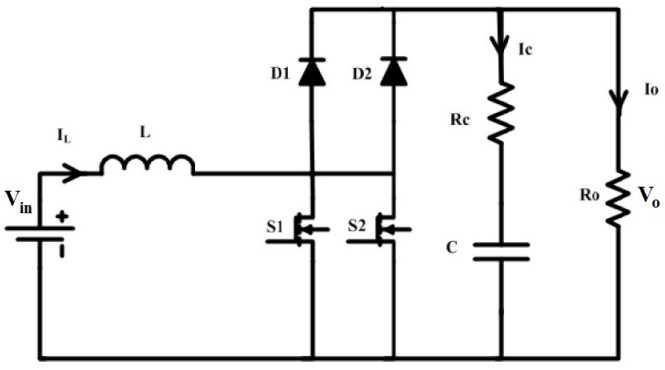

Fig. 1. Compact Boost Converter

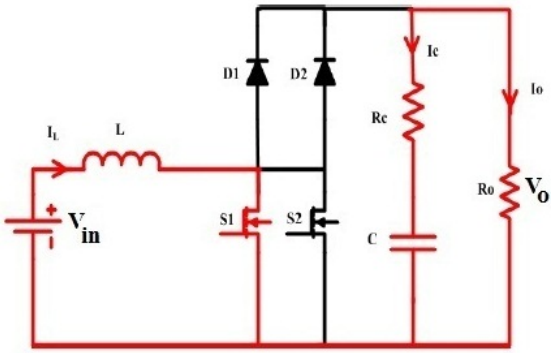

Fig. 3. Mode 1 : S_1 - ON and S_2 - OFF

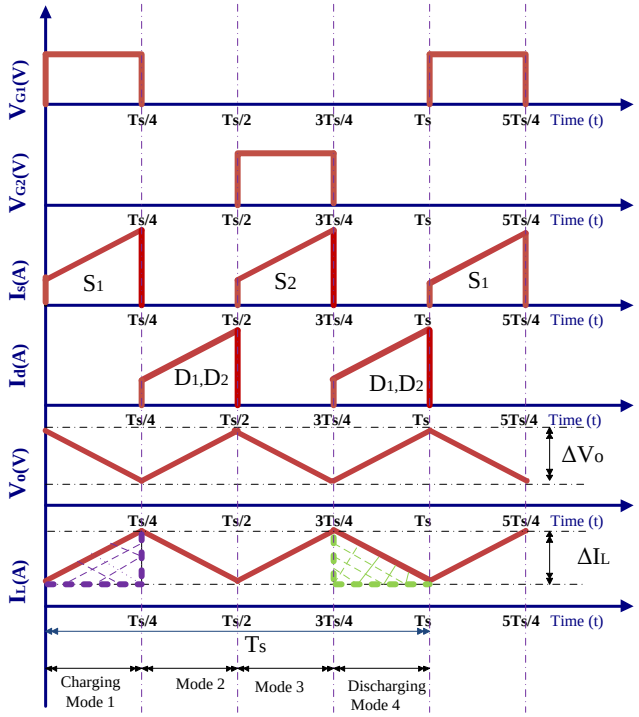

Fig. 2. Waveforms for CBC

A. Charging Modes

In Mode I and Mode III , either the switch S_1 / S_2 is turned ON and the other switch is turned OFF. The equivalent circuits are given in Fig.3 and 4. The differential equations are derived for the charging modes and is shown in (1) and (2).

$$L\frac{dI_L}{dt} = V_{in} \tag{1}$$

$$C\frac{dV_C}{dt} = \frac{-V_o}{R} \tag{2}$$

B. Discharging Modes

Both the switches S_1 and S_2 are turned OFF in discharging modes. The energy stored in the inductor is delivered to the capacitor, C during modes 2 and 4. The equivalent circuit

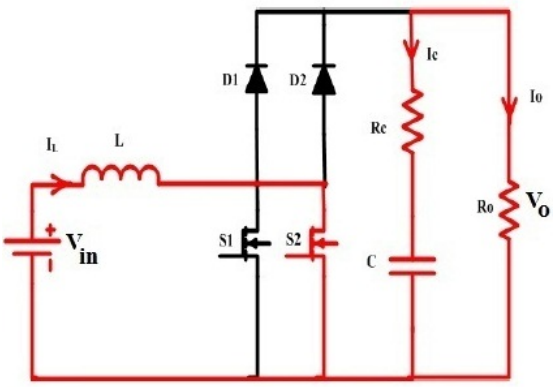

Fig. 4. Mode 3 : S_1 - OFF and S_2 - ON

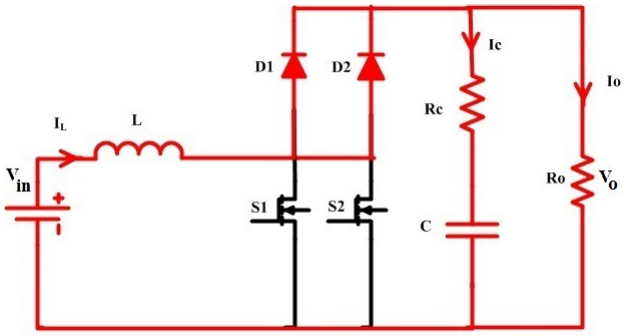

Fig. 5. Mode 2 and 4 : S_1 - OFF and S_2 - OFF

for these modes are same and is in Fig 5. The equations for discharging modes are given in Eqns.(3) and (4).

$$L\frac{dI_L}{dt} = V_{in} - V_o \tag{3}$$

$$C\frac{dV_C}{dt} = I_L - \frac{V_o}{R} \tag{4}$$

III. Design of CBC

The duration of each mode is related to the switching period ,Ts. The inductor is charged and discharged twice for one switching period. The expression for voltage gain is obtained by equating volt-sec balance of inductor.

$$\frac{V_{in}}{L}t_1 = \frac{V_o - V_{in}}{L}t_2 \tag{5}$$

where, $t_1 = \frac{DT_s}{4}$ and $t_2 = \frac{(1-DT_s)}{4}$.

$$\frac{V_o}{V_{in}} = \frac{2}{2-D} \tag{6}$$

Equation (6) is for CBC with two parallel paths. The generalized equation for voltage gain with m parallel paths is given as

$$\frac{V_o}{V_{in}} = \frac{m}{m-D} \tag{7}$$

Similarly, the current gain for the converter is,

$$\frac{I_{in}}{I_o} = \frac{m}{m-D} \tag{8}$$

TABLE II
COMPARISON OF BC AND CBC

Parameters	Boost Converter	Compact Boost Converter
V_{in} (V)	24	24
V_o(V)	84	84
I_o(A)	4.8	4.8
ΔV (V)	0.52	0.21
ΔI (A)	0.96	0.48
F (kHz)	30	30
R (Ω)	17.5	17.5
C (μF)	220	100
L (μH)	590	295
$R_L(m\Omega)$	210	105
D (%)	71	35
$R_c(m\Omega)$	0.697	1.394

The expression for current ripple (ΔI_L) is derived by obtaining slope of I_L from Modes 1 and 2.

$$\frac{T_s}{2} = \frac{\Delta I_L}{V_{in}} + \frac{\Delta I_L}{V_o - V_{in}} \tag{9}$$

$$\Delta I_L = \frac{DV_{in}}{mLf_s} \tag{10}$$

The voltage ripple (ΔV_C) in capacitor is obtained from the current flowing through it.

$$\Delta V_C = \int_0^{\frac{T_s}{4}} I_0 dt \tag{11}$$

$$\Delta V_C = \frac{DI_o}{mCf_s} \tag{12}$$

The design equations of L and C are derived for CBC and is given in comparison with BC in Table I.

TABLE I
DESIGN FORMULAE

BC	CBC
$L = \frac{D*V_{in}}{\triangle I_L * f_s}$	$L = \frac{D*V_{in}}{m*\triangle I_L * f_s}$
$C = \frac{D*I_o}{f_s*\triangle V_C}$	$C = \frac{D*I_o}{m*f_s*\triangle V_C}$
$V_0 = \frac{V_{in}}{1-D}$	$V_0 = \frac{m*V_{in}}{m-D}$
$I_0 = I_{in} * (1-D)$	$I_0 = I_{in} * \frac{(m-D)}{m}$

The design formulae is used to choose appropriate design specifications for both of the converters. The values are listed in Table II. From Table II , it is visible that for the same input and output rating, the size of passive devices like inductor and capacitor is reduced for CBC. In addition the stress across the switch is reduced as the switch is ON for half the time than that of conventional converter.

IV. MATHEMATICAL MODELLING OF CBC

Small Signal Modelling (SSM) [20]–[22] is used to derive the mathematical model of DC/DC Converters. The converter is operated in four modes and in each mode ,the circuit is assumed to be a linear time invariant system. The state space representation of LTI system is given in Eqns.(12) and (13). The averaged state model takes the form as described below.

$$\hat{X} = [A][X] + [B][Vin] \tag{13}$$

$$V_o = [C][X] + [D][Vin] \tag{14}$$

X and V_{in} are the averaged state and input variables respectively. The A ,B,C and E matrices are the weighted averages of actual matrices describing the modes of the converter. The system gain matrices for CBC are

$$A_1 = A_3 = \begin{bmatrix} 0 & 0 \\ 0 & \frac{-1}{RC} \end{bmatrix} \; ; \; A_2 = A_4 = \begin{bmatrix} 0 & \frac{-1}{L} \\ \frac{1}{C} & \frac{-1}{RC} \end{bmatrix}$$

$$B_1 = B_2 = B_3 = B_4 = \begin{bmatrix} \frac{1}{L} \\ 0 \end{bmatrix}$$

$$C_1 = C_2 = C_3 = C_4 = \begin{bmatrix} 0 & 1 \end{bmatrix}$$

$$E_1 = E_2 = E_3 = E_4 = \begin{bmatrix} 0 \end{bmatrix}$$

Assuming time varying quantities for input and duty ratio to produce pertubations on dynamic variables x and v_o in Eqns.(12)and (13), the linear model for the CBC is derived. The linear equations are given as

$$\hat{x} = A\hat{x} + B\hat{v_{in}} + f\hat{d} \tag{15}$$

$$v_o = C\hat{x} \tag{16}$$

where f is given by,

$$f = [(A_1 - A_2 - A_4)X + (B_1 - B_2 - B_4)V_{in})]\hat{d} \tag{17}$$

$$X = A^{-1}BV_{in} \tag{18}$$

From the above linear SSM as in (17)-(20), the control transfer functions namelyG_{vd} and G_{id} for resistive load is derived for CBC and are given in (21)and (22).

$$G_{vd} = \frac{V_{in}}{2R(1-D)^2}\left[\frac{1 + s(2RL(1-D)^3)}{\frac{LCs^2}{4(1-D)^6} + \frac{sL}{2R(1-D)^3} + 1}\right] \tag{19}$$

$$G_{id} = \frac{V_{in}}{4(1-D)}\left[\frac{1 + \frac{sRC}{4(1-D)}}{\frac{LCs^2}{4(1-D)^6} + \frac{sL}{2R(1-D)^3} + 1}\right] \tag{20}$$

V. Design of PID controller

The control transfer functions derived using SSM are used to design linear controllers of DC/DC Converters [23]–[25]. The transfer functions are discretized using one of the indirect digital control method namely Zero-Order Hold (ZOH). The resultant discrete transfer function is used to design digital controller $G_c(z)$ for the converter. The digital controller is designed by using bode-diagram in discrete time domain based on required gain and phase margin. By Euler method, the general structure of PID controller is given in Eqn.(25).

$$G_c(s) = K_p + K_i\frac{T_s}{z-1} + K_d\Big(\frac{N}{1+\frac{N}{1+\frac{z-1}{T_s}}}\Big) \tag{21}$$

$$\tag{22}$$

where, where, The gain constants are

$$K_p = \frac{cos\theta}{|G_{ol}(z)|} \tag{23}$$

$$K_i = \frac{-\omega_{cz}}{|G_{ol}(z)|} \tag{24}$$

$$K_d = \frac{\omega_{cz}}{|G_{ol}(z)|} \tag{25}$$

$$\theta = 180^\circ - \theta_m - \angle|G_{oz}| \tag{26}$$

The G_{ol} is the discrete time transfer function of open loop system. ϕ_m is the required phase margin , ω_{cz} is the critical frequency, Ts is the sampling time and N is the derivative filter. The control transfer functions are given as input in the SISO tool of MATLAB/simulink. The SISO tool is used to design a PID controller. The controllers coefficient values are obtained using from the transfer function Gc(z) in MATLAB. These coefficient values are used to generate gate pulses using Arduino board. The uncompensated and compensated bode plot for CBC is given in Fig.7. The uncompensated converter system has a gain margin of 29.9 dB and a phase margin of 144° whereas the gain margin and phase margin for the voltage controlled compensated loop are 69.8 dB and 62° respectively.The PID coefficients of the controller from SISO tool is listed in Table III. These coefficient values are given to the PID alogorithm of Arduino board , so as to generate the gate pulses.

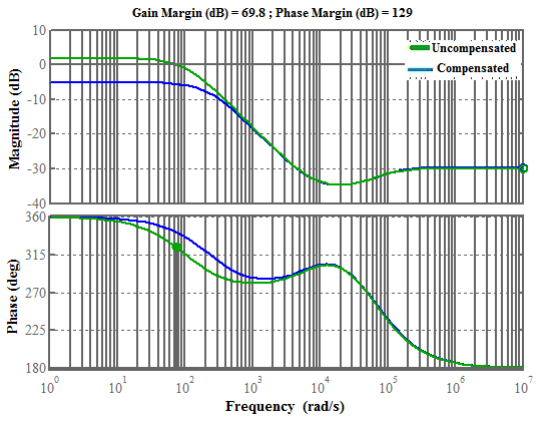

Fig. 6. Uncompensated and Compensated Bode Plots

The PID coefficients of the controller from SISO tool is listed in Table IV.

TABLE III
PID coefficients of CBC

S.No	PID Co-efficients	Value
1.	K_p	201.97
2.	K_i	434.7
3.	K_d	117.6
4.	N	1

VI. Experimental results

An hardware prototype is developed for BC and CBC. The converters are designed for same input and output power. The experimental setup is shown in Fig.8. The designed parameter values and the experimental parameter values are almost the same. The Part Nos of the components are listed in Table IV.

TABLE IV
Part Nos of Components used In Prototype

Devices	BC	CBC
MOSFET	IRF840	
Diode	MUR840	
Inductors	BWLX3015A-511	BWLX3020A-311
Capacitor	SKR221M2AK25M	CE13C11H
Driver	TLP250	

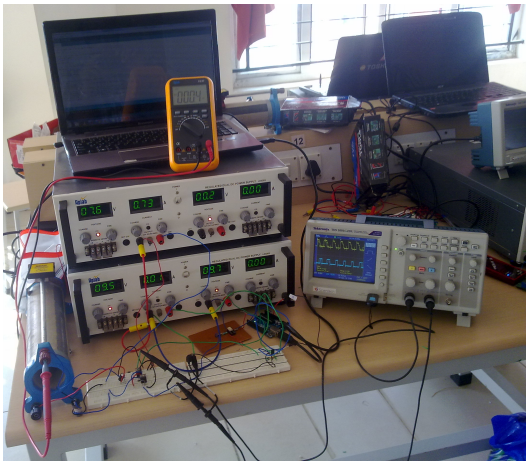

Fig. 7. Experimental Setup for BC and CBC

Arduino, an open source hardware and software, is used for designing the closed loop control. ATMega328 microcontroller is used in Arduino board. It is capable of generating pulses of frequency up to 62.50 kHz. There are six analog I/O pins and 6 PWM output pins in it. The feedback voltage is given

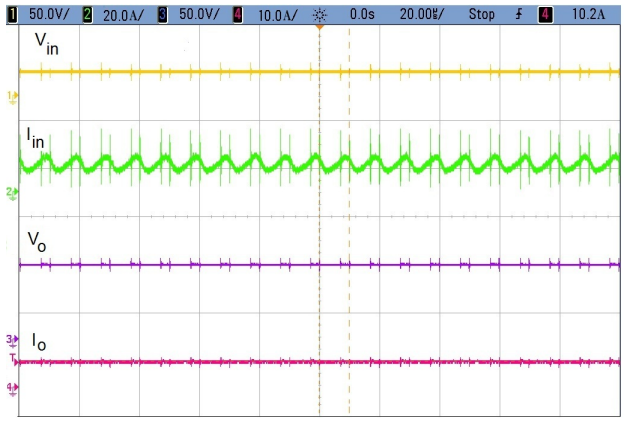

Fig. 8. Output Waveforms of Boost Converter

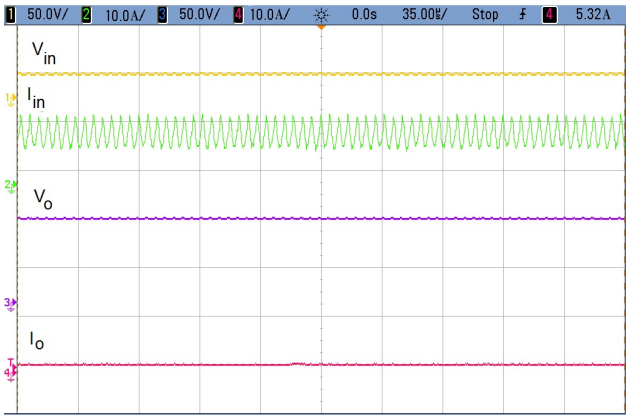

Fig. 9. Output Waveforms of Compact Boost Converter

through this analog pin and PWM signal is generated from the PWM pins. The Arduino is programmed with the open source Arduino software and the controller is powered through a USB cable. TLP250 is used as driver for MOSFET. The load of 17.5 Ω is used. Voltage divider is used at the output side of the converter to get feedback voltage. The value of R_1 and R_2 are set by equation of voltage division.

Phase correct PWM capability of ATMega328 is used to control the output voltage. The feedback voltage is taken from the converter and is given to given to analog pin1. It is converted to digital by internal ADC. This digital value is processed through PID algorithm where the set Kp,Ki and Kd values are manipulated and PWM pulses is generated at the output pin 11 and pin 12. An input of 24V is given to the converter.The voltage closed loop is implemented using PID control algorithm of microcontroller. In this algorithm the PWM signal is generated according to the PID co-efficient values.The output results are taken on MSO for both of the converters. The output of BC and CBC are shown in Fig.9 and Fig.10. The gate pulses and inductor current waveform of CBC are given in Fig.11 . The load resistance is changed from from 12Ω to 20Ω . The output voltage waveforms are observed in closed loop using Aurdino. From the waveforms it is clear that, the output voltage of converter is regulated by the microcontroller for change in load resistance.

The input and output current and voltages are measured for

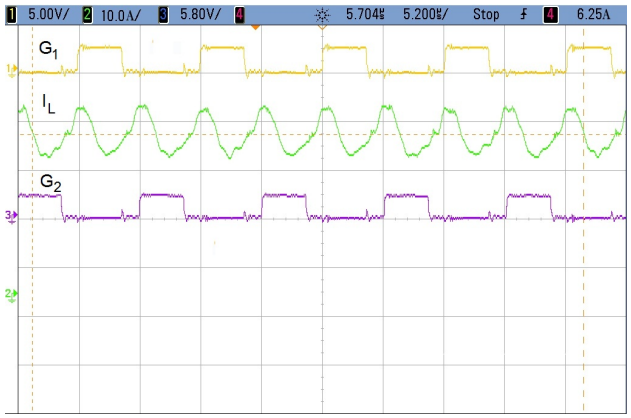

Fig. 10. Gate pulses and Inductor Current waveform of closed loop CBC

both of the converters for by varying the load. The efficiency curve is plotted for load change and is shown in Fig.12. From Fig.12, it is evident that the efficiency of CBC is greater than BC.

TABLE V
HARDWARE RESULTS BC AND CBC

Parameters	Boost Converter	Compact Boost Converter
V_{in} (V)	24.23	24.23
F (kHz)	31.25	31.25
V_o(V)	81.8	81.8
I_o(A)	4.6	4.7
ΔV (V)	0.6	0.31
ΔI (A)	1.1	0.56

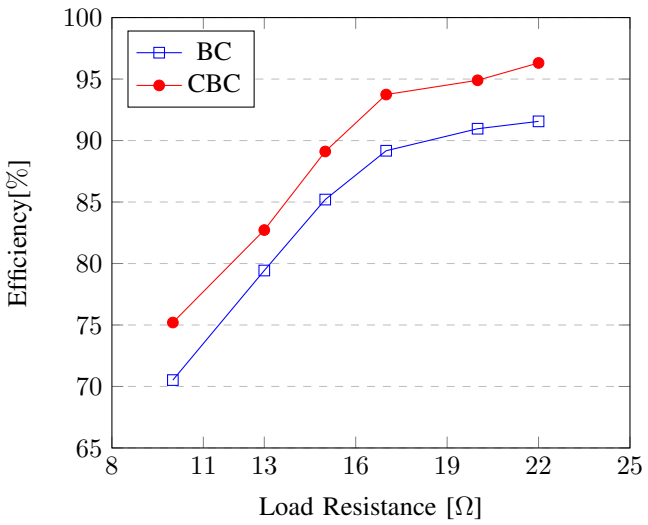

Fig. 11. Load change Vs Efficiency - BC, CBC

VII. Conclusion

The design of CBC is done and compared with BC. From the design equations it is clear that, the size of the passive components in CBC is reduced to half than BC. The control transfer functions for CBC is derived so as to develop a closed loop model using Aurduino board. An experimental prototype is developed for CBC and BC. The prototype is tested for load variations. It is observed from the hardware results, the voltage and current ripple is reduced for CBC with an increase in efficiency . This converter can be used in solar based renewable energy systems, Electric vehicles etc.,

References

[1] X. Lu, K. Sun, J. M. Guerrero, J. C. Vasquez, and L. Huang, "State-of-charge balance using adaptive droop control for distributed energy storage systems in dc microgrid applications," *IEEE Transactions on Industrial electronics*, vol. 61, no. 6, pp. 2804–2815, 2014.

[2] Y. Du and D. D.-C. Lu, "Battery-integrated boost converter utilizing distributed mppt configuration for photovoltaic systems," *Solar energy*, vol. 85, no. 9, pp. 1992–2002, 2011.

[3] X. Tan, Q. Li, and H. Wang, "Advances and trends of energy storage technology in microgrid," *International Journal of Electrical Power & Energy Systems*, vol. 44, no. 1, pp. 179–191, 2013.

[4] W. Li and X. He, "Review of nonisolated high-step-up dc/dc converters in photovoltaic grid-connected applications," *IEEE Transactions on Industrial Electronics*, vol. 58, no. 4, pp. 1239–1250, 2011.

[5] W. Yu, H. Qian, and J.-S. Lai, "Design of high-efficiency bidirectional dc–dc converter and high-precision efficiency measurement," *IEEE Transactions on Power Electronics*, vol. 25, no. 3, pp. 650–658, 2010.

[6] W. Li and X. He, "Review of nonisolated high-step-up dc/dc converters in photovoltaic grid-connected applications," *IEEE Transactions on Industrial Electronics*, vol. 58, no. 4, pp. 1239–1250, 2011.

[7] Y. Xue, L. Chang, S. B. Kjaer, J. Bordonau, and T. Shimizu, "Topologies of single-phase inverters for small distributed power generators: an overview," *IEEE Transactions on Power Electronics*, vol. 19, no. 5, pp. 1305–1314, 2004.

[8] H. Nafisi, S. M. M. Agah, H. A. Abyaneh, and M. Abedi, "Two-stage optimization method for energy loss minimization in microgrid based on smart power management scheme of phevs," *IEEE Transactions on Smart Grid*, vol. 7, no. 3, pp. 1268–1276, 2016.

[9] Y. Lu, H. Wu, K. Sun, and Y. Xing, "A family of isolated buck-boost converters based on semiactive rectifiers for high-output voltage applications," *IEEE Transactions on Power Electronics*, vol. 31, no. 9, pp. 6327–6340, 2016.

[10] L. Yan and B. Lehman, "An integrated magnetic isolated two-inductor boost converter: analysis, design and experimentation," *IEEE transactions on power electronics*, vol. 20, no. 2, pp. 332–342, 2005.

[11] M. Muhammad, M. Armstrong, and M. Elgendy, "Non-isolated, high gain, boost converter for power electronic applications," 2016.

[12] G. A. Henn, R. Silva, P. P. Praça, L. H. Barreto, and D. S. Oliveira, "Interleaved-boost converter with high voltage gain," *IEEE Transactions on Power Electronics*, vol. 25, no. 11, pp. 2753–2761, 2010.

[13] M. M. Peretz and S. Ben-Yaakov, "Time-domain design of digital compensators for pwm dc-dc converters," *IEEE Transactions on Power Electronics*, vol. 27, no. 1, pp. 284–293, 2012.

[14] V. Arikatla and J. A. A. Qahouq, "Dc-dc power converter with digital pid controller," in *Applied Power Electronics Conference and Exposition (APEC), 2011 Twenty-Sixth Annual IEEE*. IEEE, 2011, pp. 327–330.

[15] N. Eghtedarpour and E. Farjah, "Control strategy for distributed integration of photovoltaic and energy storage systems in dc micro-grids," *Renewable energy*, vol. 45, pp. 96–110, 2012.

[16] Y.-J. Lee and A. Emadi, "Phase shift switching scheme for dc/dc boost converter with switches in parallel," in *2008 IEEE Vehicle Power and Propulsion Conference*. IEEE, 2008, pp. 1–6.

[17] F. Nejabatkhah, S. Danyali, S. H. Hosseini, M. Sabahi, and S. M. Niapour, "Modeling and control of a new three-input dc–dc boost converter for hybrid pv/fc/battery power system," *IEEE Transactions on power electronics*, vol. 27, no. 5, pp. 2309–2324, 2012.

[18] P. Garcia, L. M. Fernandez, C. A. Garcia, and F. Jurado, "Energy management system of fuel-cell-battery hybrid tramway," *IEEE Transactions on Industrial Electronics*, vol. 57, no. 12, pp. 4013–4023, 2010.

[19] B. Beauregard, "Pidlibrary," *Retrieved from Arduino Playground: http://playground. arduino. cc/Code/PIDLibrary*, 2013.

[20] R. Middlebrook, "Small-signal modeling of pulse-width modulated switched-mode power converters," *Proceedings of the IEEE*, vol. 76, no. 4, pp. 343–354, 1988.

[21] S. Chander, P. Agarwal, and I. Gupta, "Design, modeling and simulation of dc-dc converter for low voltage applications," in *2010 IEEE International Conference on Sustainable Energy Technologies (ICSET)*. IEEE, 2010, pp. 1–6.

[22] ——, "Auto-tuned, discrete pid controller for dc-dc converter for fast transient response," in *India International Conference on Power Electronics 2010 (IICPE2010)*. IEEE, 2011, pp. 1–7.

[23] R. Shenbagalakshmi and T. S. R. Raja, "Modelling and simulation of digital compensation technique for dc–dc converter by pole placement," *Journal of The Institution of Engineers (India): Series B*, vol. 96, no. 3, pp. 265–271, 2015.

[24] S. Buso and P. Mattavelli, "Digital control in power electronics," *Lectures on power electronics*, vol. 1, no. 1, pp. 1–158, 2006.

[25] D. Maksimovic, R. Zane, and R. Erickson, "Impact of digital control in power electronics," in *Power Semiconductor Devices and ICs, 2004. Proceedings. ISPSD'04. The 16th International Symposium on*. IEEE, 2004, pp. 13–22.